ISSN 0023-1584, Kinetics and Catalysis, 2009, Vol. 50, No. 2, pp. 284–296. © Pleiades Publishing, Ltd., 2009.
Original Russian Text © V.I. Anikeev, 2009, published in Kinetika i Kataliz, 2009, Vol. 50, No. 2, pp. 300–313.

FIFTY YEARS
OF THE BORESKOV INSTITUTE OF CATALYSIS

Transformations of Organic Compounds in Supercritical Fluid Solvents: From Experiments to Kinetics, Thermodynamics, Simulation, and Practical Applications

V. I. Anikeev

Boreskov Institute of Catalysis, Siberian Branch, Russian Academy of Sciences, Novosibirsk, 630090 Russia
e-mail: anik@catalysis.nsk.su

Received March 28, 2008

Abstract—The results of fundamental studies performed by the author on the reactivity of supercritical fluid solvents are systematized and generalized; practical applications of these solvents are considered. Methods for performing kinetic and physicochemical experiments, processing the data, constructing kinetic models, and calculating the thermodynamics of nonideal supercritical fluids (the parameters of critical points, binodal and spinodal lines, and critical point drifts; the thermophysical properties of reaction mixtures under supercritical conditions; etc.) are described. Attention is focused on the effect of supercritical fluid pressure on the rate constants of chemical reactions. The kinetics and mechanisms of the reactions of 2-propanol dehydration and decomposition of aliphatic nitro compounds in supercritical water and the isomerization of terpene compounds (α-pinene, β-pinene, and turpentine) in supercritical lower alcohols are studied. The formation of nanoparticles in supercritical fluid solvents and the treatment of ultradisperse diamonds in supercritical water are considered. The results formed the basis for the simulation and calculation of acetic acid and phenol oxidation processes in supercritical water and the Fischer–Tropsch synthesis in a supercritical solvent and for the development of a pilot plant for the complete oxidation of trinitroglycerol and diethylene glycol dinitrate in supercritical water.

DOI: 10.1134/S0023158409020207

INTRODUCTION

The properties of supercritical fluid (SCF) solvents, such as heat capacity, heat conductivity, and diffusion near the critical point, change significantly under slight temperature and pressure variations. Because of this, they are attractive for performing many chemical processes, including heterogeneous chemical reactions (the synthesis, isomerization, hydrogenation, decomposition, and oxidation of organic compounds), and promising for the development of new technologies on their basis [1, 2]. SCFs find practical applications in extraction and oxidation processes, waste utilization, waste processing, biomass and coal conversion, organic synthesis, the development of new materials (including nanomaterials), etc. [3, 4].

In this review, both the results of fundamental studies on the reactivity of SCFs (including methods for performing kinetic experiments, data processing, constructing kinetic models, studying the thermodynamics of nonideal fluids, mathematical modeling, and the determination of the role of pressure) and problems related to the practical implementation of processes for the deep oxidation of organic compounds in supercritical water are surveyed and systematized.

EXPERIMENTAL INVESTIGATION TECHNIQUES

The transformations of organic compounds in SCF solvents were studied in reactors of the following two types: autoclave reactors and flow tube reactors [5, 6]. The autoclave reactors, which were designed for operation under high pressures (the maximum working pressure at 500°C was ~430 atm), were equipped with magnetic stirrers and a specially developed injection and microsampling system.

Systems with tubular flow reactors included micropumps for supplying several separate reagent flows, mixers, and heat exchangers.

The following requirements were taken into consideration in choosing the design of the setup, injection and sampling systems for reaction products, and experimental procedures: first, chemical transformations of a reactant before its supply to the reactor should be avoided; second, small amounts of a reactant should be supplied to the reactor with a high precision; third, flows should be mixed and heated to a specified temperature in a short time; fourth, the state of the reaction medium in the reactor should remain unchanged in the course of sampling. Hewlett-Packard 5890-17, 5890/II, and 6890 chromatographs with various columns and detectors were used to analyze reaction products.

METHODS FOR PROCESSING EXPERIMENTAL DATA AND CONSTRUCTING KINETIC MODELS

As a rule, models like the following set of ordinary differential equations were used for processing experimental data obtained in the plug-flow reactor and for determining the constants of rate equations:

$$\frac{dy_i}{d\tau} = \sum_{j=1}^{N_R} z_{ji} R_j(y), \quad (1)$$

where $y_i = C_i/C_i^0$ (C_i and C_i^0 are the current and initial concentrations of the ith component, respectively), N_R is the number of chemical reactions included in the reaction scheme, z_{ji} is the number designating the jth row and the ith column of the stoichiometric matrix corresponding to the reaction scheme, τ is the contact time, and $R_j(y)$ is the first-order reaction rate. At $\tau = 0$, $y_1^0 = 1$, $y_i^0 = 0$, and $i = 2, \ldots, N_S$. (Here, N_S is the number of components.) The identification problem implies the determination of unknown rate constants and activation energies at which the best fit between experimental and calculated data is obtained. For this purpose, an objective function is formulated to be minimized with respect to parameters

$$Q = \sum_{k=1}^{N_{expt}} (\mathbf{y}_k^{expt} - \mathbf{y}_k^{calcd}(\mathbf{p}))^T \times \mathbf{W}_k^{-1} (\mathbf{y}_k^{expt} - \mathbf{y}_k^{calcd}(\mathbf{p})) \longrightarrow \min(\mathbf{p}), \quad (2)$$

where $\mathbf{y}_k^{expt}$ is the N_S-dimensional column vector of experimentally measured concentrations of the ith component in each particular kth experiment; $\mathbf{y}_k^{calcd}$ is the vector of calculated concentrations obtained by the integration of the set of differential equations of model (1) between the limits of 0–τ (s) at the corresponding temperature in the kth experiment (T_k); $\mathbf{W}_k$ is the weight unit matrix; and $\mathbf{p}$ is the N_P-dimensional column vector of the desired parameters having the form

$$\mathbf{p} = [k_{10}, k_{20}, \ldots, k_{40}, E_1, E_2, \ldots, E_4]. \quad (3)$$

The minimization of objective function (2) was performed using the classical Gauss–Marquardt iteration method [7]. The concentrations were calculated in each iteration step by numerical integration of the set of differential equations (1) at the current values of the constants. The identification procedure and the statistical analysis of the reliability of the results were described in detail elsewhere [8].

THERMODYNAMICS OF SUBCRITICAL AND SUPERCRITICAL REACTION MIXTURES

The calculation of the phase equilibrium of multicomponent mixtures in the subcritical region and the thermodynamic properties of the mixtures in the supercritical region was an integral part of the study of the test systems. Ideal gas or solution laws, which imply the mutual energetic independence of mixture components, are not applicable to subcritical and supercritical mixtures. Therefore, the state of a reaction mixture is calculated with the use of two-parameter cubic equations of state, for example, the Redlich–Kwong–Soave (RKS), Peng–Robinson, and Patel–Teja equations.

Equation of state. To calculate the phase states and the thermodynamic and thermophysical properties of multicomponent mixtures, we used the RKS equation of state [9]

$$P = \frac{RT}{V_m - b_m} - \frac{a_m(T)}{V_m(V_m + b_m)}, \quad (4)$$

where V_m is the molar volume of the mixture (l/mol). The coefficients a_m and b_m for a mixture with the specified molar composition vector $\mathbf{y}$ were determined as follows:

$$a_m = \sum_{j=1}^{N_s}\sum_{i=1}^{N_s} y_i y_j a_{ij}, \quad b_m = \sum_{j=1}^{N_s}\sum_{i=1}^{N_s} y_i y_j b_{ij}; \quad (5)$$

$$a_{ii} = \alpha_i(T)(0.42748 R^2 T_{i,кр}^2/P_{i,cr}), \quad b_{ii} = 0.08664 R T_{i,cr}/P_{i,cr}; \quad (6)$$

$$a_{ij} = (1 - k_{ij})\sqrt{a_{ii}a_{jj}}, \quad b_{ij} = (1 - c_{ij})(b_{ii} + b_{jj})/2, \quad \alpha_i(T) = [1 + d_i(1 - \sqrt{T/T_{i,cr}})]^2; \quad (7)$$

$$d_i = 0.480 + 1.574\omega_i - 0.176\omega_i^2.$$

The critical temperature and pressure of the ith mixture component are denoted by $T_{i,cr}$ and $P_{i,cr}$, respectively. The parameter ω_i, which is referred to as an acentric factor, is given in thermochemical handbooks. The quantities k_{ij} and c_{ij} are binary interaction coefficients. The accuracy of the calculations of phase diagrams and critical parameters of complex mixtures mainly depends on the correct choice or calculation of the binary interaction coefficients k_{ij} and c_{ij} in Eqs. (7). In this context, a procedure for the determination of k_{ij} and c_{ij} was proposed [10] with consideration for the temperature and pressure dependence of these coefficients.

Equations for the calculation of partial molar volumes. By definition, the partial molar volume of the ith mixture component is calculated from the following relationship:

$$\bar{V}_i = \left[\frac{\partial(nV_m)}{\partial n_i}\right]_{P,T,n_j} = V_m + \frac{\partial V_m}{\partial y_i}(1 - y_i), \quad (8)$$

where V_m is the molar volume of the mixture; n_i and y_i are the number of moles and the mole fraction of the ith

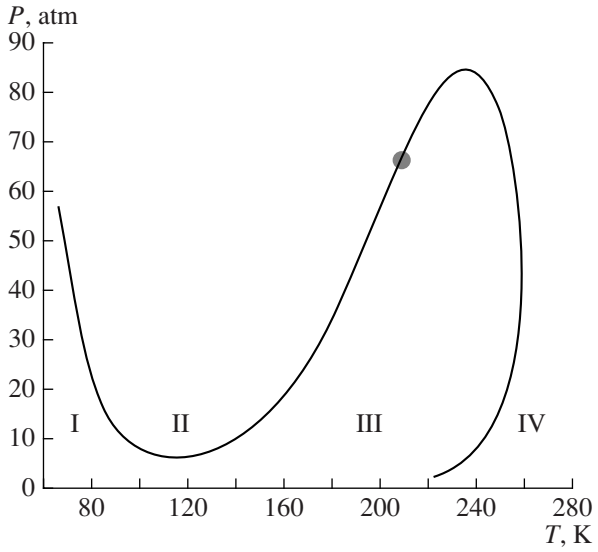

Fig. 1. Binodal line in the *P–T* plane and the critical point for a model mixture containing 0.15 mol % He, 3.4 mol % N_2, 86.4 mol % CH_4, 6.5 mol % C_2H_6, 3.0 mol % C_3H_8, and 0.55 mol % C_5H_{12}: (I) two-phase solid–gas region, (II) homogeneous liquid phase region, (III) two-phase gas–liquid region, and (IV) homogeneous gas phase region.

component of the mixture; and $n = \sum_i n_i$ is the total number of moles in the mixture. Here,

$$\frac{\partial V_m}{\partial y_i} = \frac{\partial P/\partial y_i}{\partial P/\partial V_m}. \quad (9)$$

Derivatives in the numerator and denominator of Eq. (9) can be found in an analytic form by differentiating Eq. (4). The partial molar volume of a solute depends strongly on both its nature and physicochemical properties and the properties of the solvent. At the same time, the partial molar volume of the solvent is actually equal to the molar volume of the mixture [11].

Model for calculating the critical point of a multicomponent mixture with a given composition. A mixture with a specified composition occurs in a critical state at a certain temperature ($T_{mix, cr}$) and pressure ($P_{mix, cr}$) at which the following conditions are satisfied simultaneously [12, 13]:

$$F_1(T, P) \equiv \mathrm{Det}(\mathbf{M}_1) = 0; \quad (10)$$

$$F_2(T, P) \equiv \mathrm{Det}(\mathbf{M}_2) = 0. \quad (11)$$

The elements of matrix $\mathbf{M}_1$ are the first derivatives of the natural logarithm of the fugacity of components with respect to the number of moles at a constant pressure and temperature:

$$\mathbf{M}_1 = \left\{\frac{\partial \ln f_i}{\partial n_j}\right\}_{T, P} \quad (12)$$

$$(i = 1, 2, \ldots, N;\ j = 1, 2, \ldots, N),$$

where N is the number of mixture components.

As a rule, the fugacity of components $f_i(T, P, \mathbf{y})$ as a function of temperature, pressure, and the molar composition of the mixture (vector $\mathbf{y}$) is calculated with the use of cubic equations of state, for example, RKS. Matrix $\mathbf{M}_2$ in Eq. (11) is obtained from matrix $\mathbf{M}_1$ by replacing any row in it with the row vector

$$[\partial F_1/\partial n_1, \partial F_1/\partial n_2, \ldots, \partial F_1/\partial n_N]. \quad (13)$$

Equation (10) describes a spinodal line in the *T–P* plane. It is monovariant and has a set of solutions with respect to the mutually dependent pair of values $T_{sp}(P_{sp})$ or $P_{sp}(T_{sp})$, which satisfy Eq. (10), for each specified mixture composition. The critical point of the mixture ($T_{mix, cr}$, $P_{mix, cr}$) is a singular point in this curve, where Eqs. (10) and (12) are satisfied simultaneously. To solve this mathematical problem, Ermakova et al. [14, 15] proposed an equivalent form of two Eqs. (10) and (12) for a critical phase to considerably simplify numerical calculations. The problem was solved by the homotopy method [16].

As an example of the calculation of a critical point and phase diagram, Fig. 1 shows the results of a study of a mixture with the following composition (mol. %): He, 0.15; C_2H_6, 6.5; N_2, 3.4; C_3H_8, 3.0; CH_4, 86.4; and C_5H_{12}, 0.55. A special feature of the location of the critical point of the mixture in the phase diagram is that its parameters $P_{cr} = 65.6$ atm and $T_{cr} = 211.2$ K are lower than the maximum values of T and P in the phase diagram.

The second example is the calculation of the position of the critical point for a mixture of benzene, cyclohexane, and hydrogen, which undergoes a considerable drift under changes in the concentration of supercritical CO_2 (Fig. 2).

Model for calculating gas–liquid, liquid–liquid, and gas–liquid–liquid phase boundaries. To calculate phase boundaries between homogeneous regions (including the supercritical region) and the regions of existence of gas–liquid and gas–liquid–liquid two- and three-phase mixtures, well-known thermodynamic models of monovariant binodal lines [17], which are also referred to as equations of tangent planes, are used. In the general case, at a fixed composition of a phase, each temperature and pressure form interdependent pairs, which minimize the function

$$F(\mathbf{x}, T, P) \equiv \frac{\Delta G}{\varepsilon RT} = \frac{1}{RT}\sum_{i=1}^{N} x_i[\ln x_i + \ln\Phi_i(x, T, P) - \ln z - \ln\Phi_i(\mathbf{z}, T, P)] \longrightarrow \min \quad (14)$$

with the constraint

$$\sum_{i=1}^{N} x_i = 1, \quad (15)$$

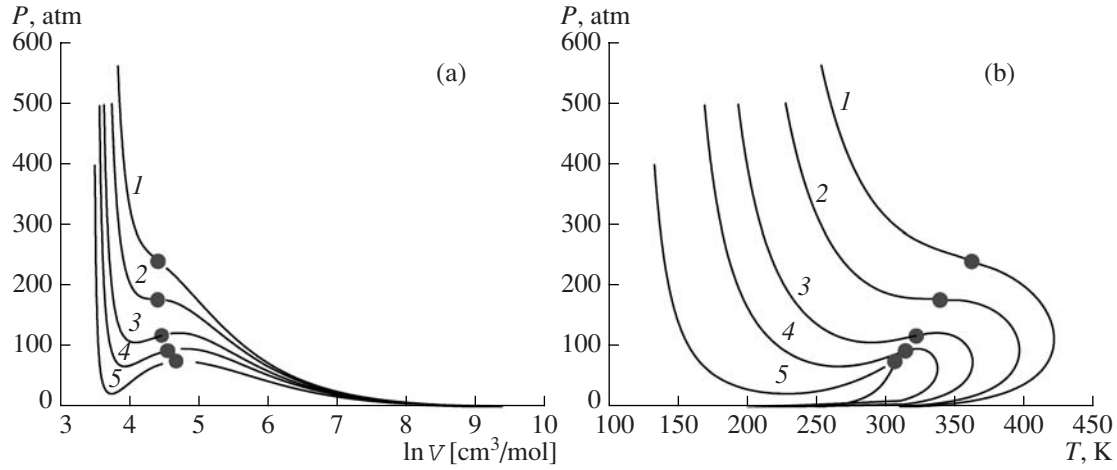

Fig. 2. Binodal lines in the (a) *P–T* and (b) *P–V* planes for mixtures containing CO_2, C_6H_6, C_6H_{12}, and H_2. Concentrations of CO_2, %: (*1*) 70, (*2*) 80, (*3*) 90, (*4*) 95, and (*5*) 99. $C_6H_6 : C_6H_{12} = 1 : 1$. $H_2 : C_6H_6 = 3 : 1$.

where ΔG is the change in the Gibbs energy as a result of the phase transition; **x** is the vector of the sought mole fractions of components formed in infinitely small amounts ε in a new equilibrium phase; **z** is the vector of the mole fractions of the starting mixture with a specified composition; $\Phi_i(\mathbf{x}, T, P)$ and $\Phi_i(\mathbf{z}, T, P)$ are the corresponding fugacity coefficients calculated from the equation of state. In this case, the following condition should be fulfilled at minimum points of function (14):

$$\mathrm{Det}[\mathbf{h}_x] > 0, \quad \mathrm{Det}[\mathbf{h}_z] > 0, \tag{16}$$

where $\mathbf{h}_x$ and $\mathbf{h}_z$ are symmetric matrices with the elements

$$\mathbf{h}_x = \left\{\frac{\partial^2 F}{\partial x_i \partial x_j}\right\}, \quad \mathbf{h}_z = \left\{\frac{\partial^2 F}{\partial z_i \partial z_j}\right\} \tag{17}$$

$$(i = 1, 2, \ldots, N;\ j = 1, 2, \ldots, N).$$

If three equilibrium phases, for example, a gas and two immiscible liquids, are formed in the system, the properties of the vapor phase can be calculated based on the known properties of either of the two liquid phases from the following phase equilibrium condition for this system:

$$f_i^{(\mathrm{liq}_1)} = f_i^{(\mathrm{liq}_2)} = f_i^{(\mathrm{vap})}. \tag{18}$$

For this purpose, equilibrium between the two liquid phases is calculated beforehand at a specified total composition of the heterogeneous liquid mixture. Separation into two liquid phases is performed in accordance with the standard flash procedure [18]. Next, with the use of model (14), the vapor composition and temperature at which conditions (14) and (15) are fulfilled are calculated at fixed pressure and liquid phase composition.

Calculation of the thermophysical properties of reaction mixtures under supercritical conditions. It is well known that, in a critical region, many thermophysical properties of a substance are changed dramatically under small temperature and pressure (density) changes. For example, the anomalous behavior of the heat capacity or thermal conductivity of water under supercritical or near-critical conditions manifests itself in the occurrence of a maximum in a curve plotted against temperature or pressure. This change in SCF properties will inevitably affect the process in a reactor. Therefore, the real changes in the properties of the mixture in the case of a process occurring in the critical region of its parameters should be taken into consideration in the simulation of reactors and apparatuses.

To calculate the heat capacity (c_p) and enthalpy (H) of individual substances in subcritical and supercritical regions, Ermakova et al. [19] used nonideal thermodynamic methods. The imperfection of the properties of individual components was taken into account with the use of the following thermodynamic functions that relate the free Gibbs energy, enthalpy, and fugacity [20]:

$$H_i = H_i^{\mathrm{id}}(T, 1) - RT^2 \frac{\partial \ln \Phi_i(T, P, \mathbf{y})}{\partial T}, \tag{19}$$

$$c_{\mathrm{p}i} = c_{\mathrm{p}i}^{\mathrm{id}}(T, 1) - R\left[2T\frac{\partial \ln \Phi_i(T, P, \mathbf{y})}{\partial T} + T^2 \frac{\partial^2 \ln \Phi_i(T, P, \mathbf{y})}{\partial T^2}\right]. \tag{20}$$

Here, $f_i = Py_i\Phi_i(T, P, \mathbf{y})$ and $\Phi_i(T, P, \mathbf{y})$ are the fugacity and fugacity coefficient of the ith mixture component, respectively; **y** is the molar composition vector of the mixture; and the superscript id indicates that this thermodynamic function calculated at P = 0.1 MPa and process temperature T corresponds to an ideal gas state. The fugacity coefficients are calculated from the RKS equation of state, whereas the first and second derivatives of the fugacity coefficients are cal-

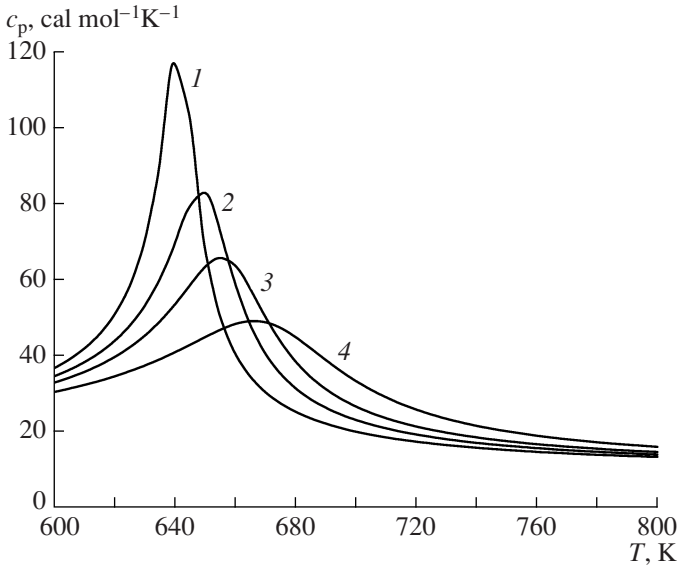

Fig. 3. The temperature dependence of the heat capacity of a mixture ($y^0_{H_2O}$ = 93.86%, y^0_{Ph} = 0.13%, y^0_{Me} = 1.57%, $y^0_{H_2O_2}$ = 1.00%, and $y^0_{O_2}$ = 3.44%) at the following pressures, atm: (*1*) 250, (*2*) 275, (*3*) 300, and (*4*) 350.

culated by numerical differentiation with respect to T at a constant P.

As an example that illustrates the importance of correct calculations of the thermophysical properties of the reaction mixture near a critical point, Fig. 3 shows the temperature dependence of the heat capacity c_p of a mixture containing water, phenol (Ph), methanol (Me), and hydrogen peroxide at various pressures. The maximum in curve *1* corresponds to the critical parameters of the mixture. As the pressure was increased, the height of the maximum of c_p decreased and the maximum shifted toward higher temperatures.

DEHYDRATION, DECOMPOSITION, AND OXIDATION REACTIONS IN SUPERCRITICAL WATER

Dehydration of 2-propanol. The kinetics and mechanism of 2-propanol dehydration in supercritical water were studied in an autoclave reactor. The experiments were performed at critical and supercritical temperatures and supercritical water densities [5, 21, 22]. Propylene, water, acetone, and propane are the main products of this reversible reaction. The reaction rate constants and activation energies were calculated from the dependence of the mole fractions of 2-propanol and propylene on the contact time. In Fig. 4, it can be seen that stable chemical equilibrium was reached some time after the onset of the reaction.

Decomposition of aliphatic nitro compounds. The reaction kinetics of decomposition and oxidation of aliphatic nitro compounds (nitromethane, nitroethane, and 1-nitropropane) in supercritical water was studied in a flow-type reactor [6, 23]. The rate constants of the reaction were calculated from experimental data (Fig. 5) on the assumption of the first-order reaction. A change in the pressure over a wide range considerably affected the rate of decomposition of the test nitrogen-containing compounds in supercritical water [24]. The reactivity of nitro compounds in decomposition reactions decreased with an increasing number of carbon atoms in the molecule, whereas the reactivity in oxidation reactions increased.

ISOMERIZATION REACTIONS OF TERPENE COMPOUNDS IN SUPERCRITICAL ALCOHOLS

The thermal isomerization of terpene hydrocarbons (turpentine, α-pinene, β-pinene, and verbenol) is a widespread method for the preparation of various polyunsaturated (diene and triene) compounds, which are

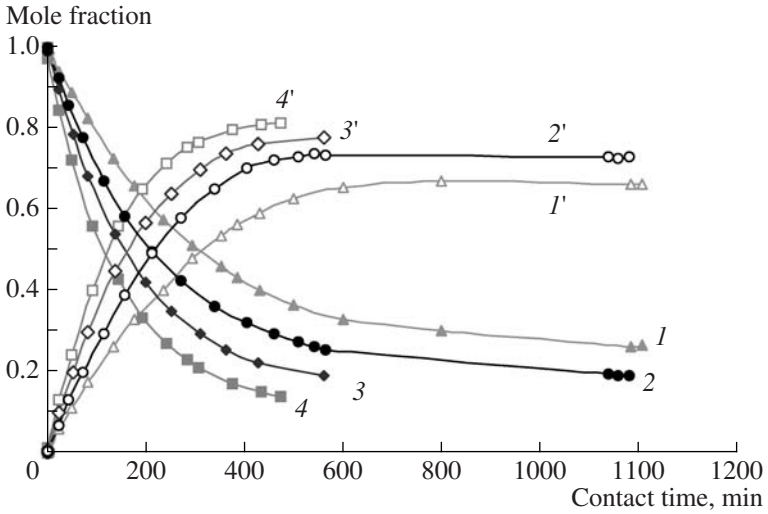

Fig. 4. Dependence of the mole fractions of (*1*–*4*) propanol and (*1*'–*4*') propylene on the residence time in the reaction of 2-propanol dehydration at the following temperatures, °C: (*1*, *1*') 381, (*2*, *2*') 393, (*3*, *3*') 403, and (*4*, *4*') 413.

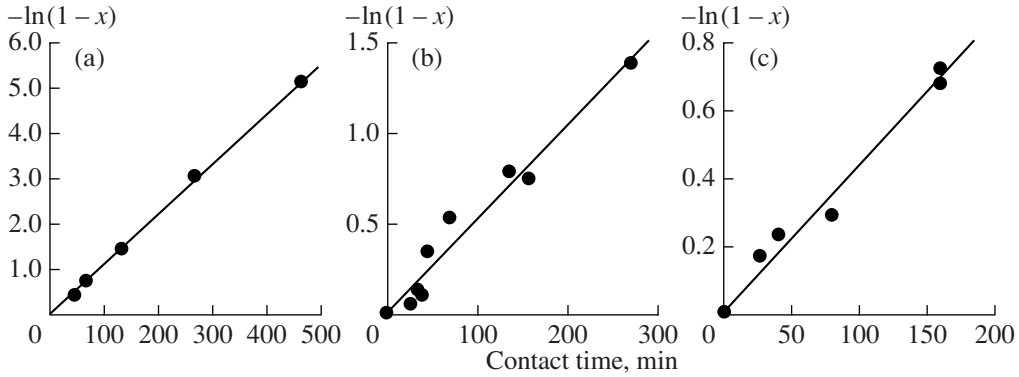

Fig. 5. Dependence of ln (1 – *x*), where *x* is the conversion, on contact time: (a) nitromethane, (b) nitroethane, and (c) 1-nitropropane.

commonly used in organic synthesis. Limonene and β-myrcene, which are key components of many essential oils extracted from plants and used as the constituents of artificial perfumes and cosmetics, are prepared by this method from bicyclic monoterpenes (α-pinene and β-pinene).

Isomerization of α-pinene in supercritical lower alcohols. Lower alcohols are commonly used as solvents for many organic compounds. They are characterized by relatively low critical parameters, and they are stable to thermal degradation in the critical region. Thus, it is of interest to use them as supercritical solvents for chemical transformations. The reaction of α-pinene isomerization was studied in methanol, ethanol, and 1-propanol [25]. Figure 6 shows the dependence of the conversion of α-pinene (curves *1*–*3*) and the formation of limonene as the main product (curves *1*'–*3*') in the above supercritical alcohols on contact time at constant temperature and pressure. The experimental results suggest the following: (1) the greater the number of carbon atoms in alcohol molecules, the higher the efficiency of alcohols as supercritical solvents; (2) the chemical composition of products obtained in the presence of all three alcohols was the same; (3) none of these supercritical alcohol solvents reacts with α-pinene and its isomerization products; and (4) none of them has a considerable effect on reaction selectivity. Limonene (the main product of α-pinene isomerization) was stable in supercritical alcohol under experimental conditions.

Various types of turpentine (turpentine oil, sulfate turpentine, and extraction turpentine) are the main source for the production of α-pinene, which is a widespread naturally occurring monoterpene hydrocarbon. Because of its ability to readily undergo various transformations and skeletal rearrangements, α-pinene serves as a starting material for the manufacture of fragrance compounds; it is also a valuable raw material for pharmaceutical industry. Our experimental results (Fig. 7) and published data [26–30] allowed us to represent the main reaction paths of α-pinene isomerization in supercritical ethanol as the following reaction scheme, which is analogous to a reaction scheme of the thermal isomerization of α-pinene in the gas or liquid phase:

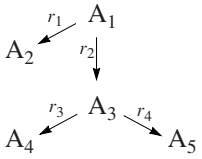

Scheme of the reaction paths of the thermal isomerization of α-pinene.

(A_1 is α-pinene, A_2 is limonene, A_3 is (4*E*, 6*Z*- + 4*E*, 6*E*-allo)ocimenes, A_4 is (α- + β-)pyronene, and A_5 are other products).

It was found that a supercritical reaction medium makes it possible to increase the rate of reaction by several orders of magnitude at an unchanged selectivity for

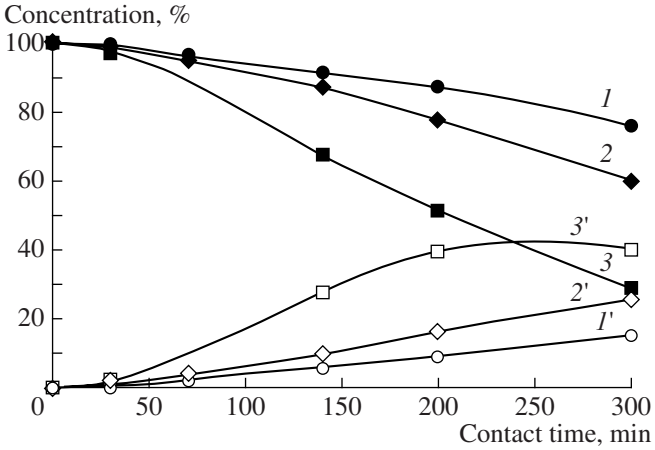

Fig. 6. Dependence of the concentrations of (*1*–*3*) α-pinene and (*1*'–*3*') limonene on contact time in the isomerization of α-pinene in supercritical alcohols at 300°C and 100 atm: (*1*, *1*') in methanol, (*2*, *2*') in ethanol, and (*3*, *3*') in 1-propanol.

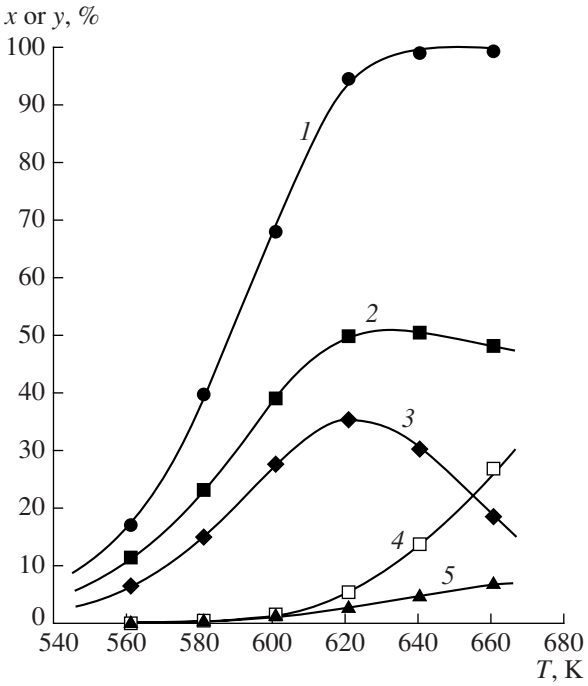

Fig. 7. The temperature dependence of (*1*) the conversion (*x*) of α-pinene and the yields (*y*) of (*2*) limonene, (*3*) 4*E*, 6*Z*-alloocimene, (*4*) 4*E*, 6*E*-alloocimene, and (*5*) (α + β)-pyronenes. Points and solid lines refer to experimental and calculated data, respectively. $P = 120$ atm.

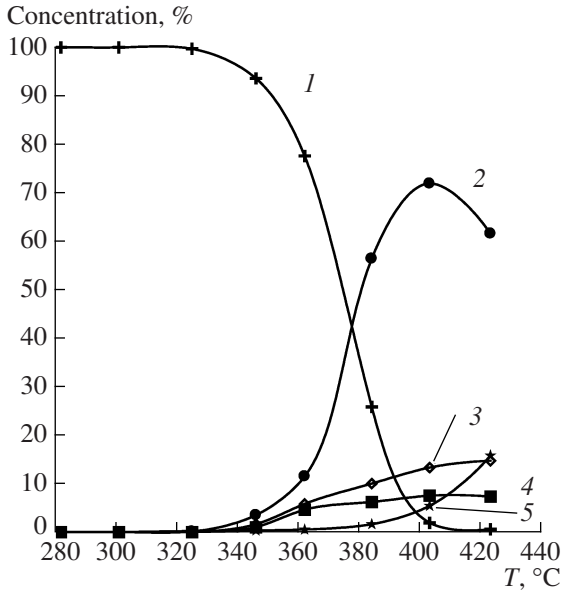

Fig. 8. Effect of temperature on the thermolysis of β-pinene in supercritical ethanol: (*1*) β-pinene, (*2*) β-myrcene, (*3*) limonene, (*4*) *para*-mentha-1(7),8-diene, and (*5*) other products. Residence time, 70 s; $P = 120$ atm; initial concentration of β-pinene, 0.1 mol/l.

the formation of limonene and alloocimene isomers. The maximum yields were 52 and 38%, respectively.

Isomerization of α-pinene in a supercritical water–ethanol solvent. We experimentally studied the effect of water as a cosolvent and catalyst for the reaction of α-pinene isomerization in a supercritical water–ethanol solvent [31]. At $T = 384$°C and $P = 230$ atm, an increase in the concentration of water in the reaction mixture resulted in an increase in the rate of reaction and the selectivity of target product (limonene) formation. Water subjected to ionization exhibited the properties of an acid catalyst. The mathematical treatment of experimental data allowed us to quantitatively evaluate and separate the contributions of radical and ionic processes to the overall rate of reactions that occur in the thermal isomerization of α-pinene.

Isomerization of β-pinene in supercritical ethanol. Our studies [32] demonstrated that the thermolysis of β-pinene in supercritical ethanol occurred at a higher temperature than that in the thermolysis of α-pinene, but the former reaction occurred over a narrower temperature range (Fig. 8). We calculated preexponential factors for the rate constants of both of the reactions and activation energies. In the reaction of β-pinene isomerization, the numerical values of these parameters were much higher. The maximum yield of β-myrcene at 400°C was as high as 72%, and the reaction performed in supercritical ethanol can be used for preparative purposes. A study of the enantiomeric composition of the thermolysis products of β-pinene, α-pinene, and limonene allowed us to better understand the mechanisms of decomposition of these monoterpenes.

EFFECT OF THE PRESSURE OF THE SUPERCRITICAL FLUID ON THE RATE CONSTANTS OF CHEMICAL REACTIONS

The dehydration of 2-propanol and the decomposition of nitro ethers in supercritical water [5, 6, 11, 24, 33, 34], as well as the isomerization of α-pinene in supercritical ethanol [30, 31], were studied. It was found that the pressure (density) of the reaction mixture considerably affects the rates of chemical reactions (rate constants) at a constant temperature (Figs. 9–11). This phenomenon is characteristic of reactions in solutions, including supercritical solvents (e.g., see [35, 36]). In the general case, the specific interaction between the solvent and reactants in it is responsible for the effect of the pressure of the supercritical solvent on the rate constant of a chemical reaction. The degree of this effect depends on both the nature and properties of the supercritical solvent and the character of the above interaction.

The effect of the density (pressure) of the supercritical solvent on the rate of chemical reactions was studied using two different approaches (models): a thermodynamic model based on the transition state theory and a model that implies that the reaction is catalyzed by the H_3O^+ ions formed because of water dissociation in the critical region. Of course, the latter model is applicable to reactions occurring in supercritical water.

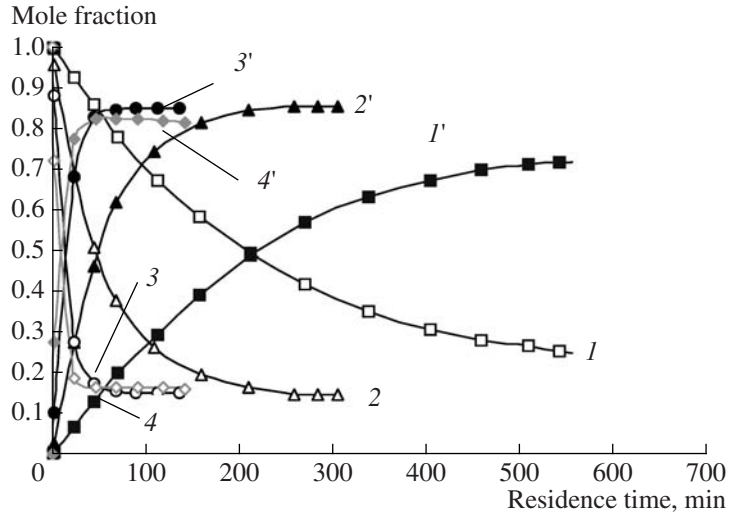

Fig. 9. Dependence of the concentrations of (*1–4*) 2-propanol and (*1'–4'*) propylene on contact time in the reaction of 2-propanol dehydration at 393°C in supercritical water with the following density, g/ml: (*1*, *1'*) 0.34, (*2*, *2'*) 0.42, (*3*, *3'*) 0.503, or (*4*, *4'*) 0.583.

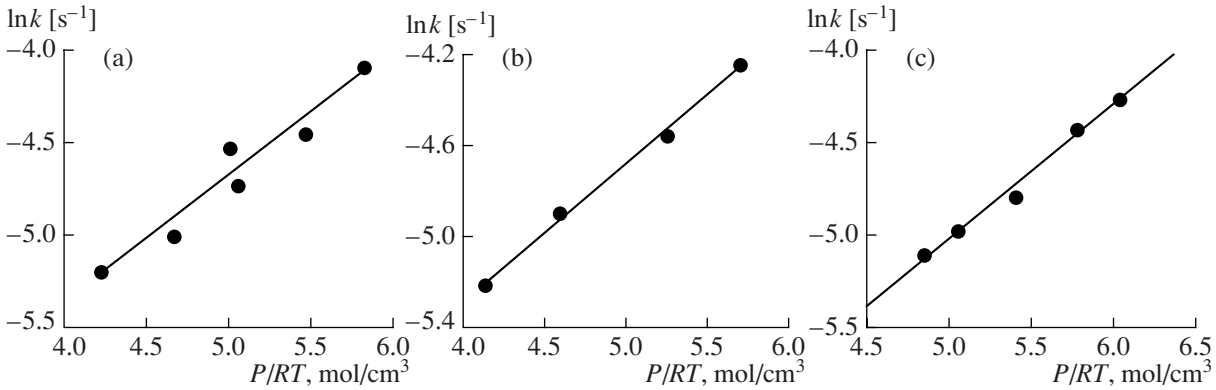

Fig. 10. The pressure dependence of the apparent reaction rate constant of decomposition of (a) nitromethane, (b) nitroethane, or (c) 1-nitropropane in supercritical water.

In terms of the former model, the nature of the activated complexes was hypothesized and their thermodynamic parameters were calculated. The transition state theory allows one to find a relationship between the rate constant of a chemical reaction and the activation volume. The activation volumes are calculated based on the experimental pressure dependences of $\ln k_{obs}$. Then, to test the adequacy of the chosen model, the activation volumes are calculated as the difference between the partial molar volumes of the transition complex and the starting reactant. To calculate the partial molar volumes of the activated complex and the starting reagent, RKS cubic equations of state are used in most cases.

With the use of the latter approach (for reactions that occur in supercritical water), it is believed that the rate of reaction is proportional to the concentration of H_3O^+ ions, which are formed as a result of water dissociation in the supercritical region and act as a homogeneous catalyst. In all of the test reactions, an increase in the concentration of H_3O^+, as the density (pressure) of supercritical water was increased, unambiguously correlated with the experimental pressure dependences of the reaction rates.

NANOPARTICLES AND ULTRADISPERSE DIAMONDS

Thermodynamics of the gas–liquid–solid equilibrium: Formation of nanoparticles in a supercritical solvent. SCFs are attractive media for the synthesis, modification, and formation of nanoparticles from inorganic and organic materials and for encapsulation. These nanostructures and materials exhibit unusual properties, which are different from those of bulk analogs. The experimental design was made based on a thermodynamic model that allowed us to calculate the equilibrium and phase states of fluid–solid systems over wide ranges of temperature, pressure, and compo-

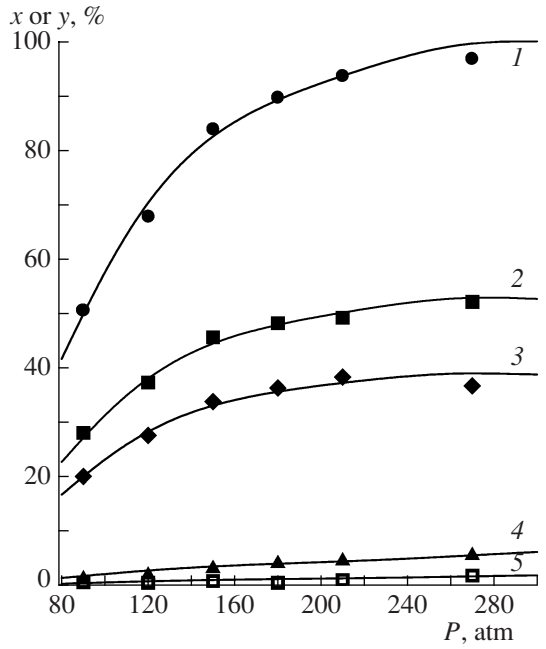

Fig. 11. The pressure dependence of (*1*) the conversion (*x*) of α-pinene in an isomerization reaction and the yields (*y*) of (*2*) limonene, (*3*) 4*E*, 6*Z* + 4*E*, 6*E*-alloocimenes, (*4*) (α + β)-pyronenes, and (*5*) other products. Points and solid lines refer to experimental and calculated data, respectively.

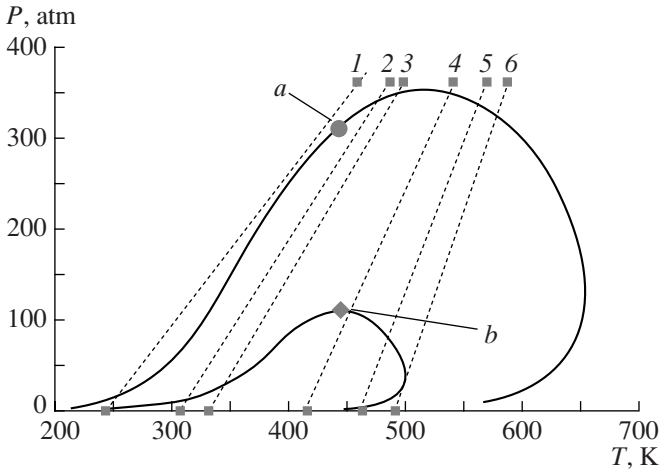

Fig. 12. Phase diagrams on the *T*–*P* plane and characteristic trajectories (dashed lines) of the adiabatic expansion of a mixture containing 5 mol % $C_{14}H_{10}$, 80 mol % CO_2, and 15 mol % C_2H_5OH. Top points *1*–*5* refer to specified initial temperatures T_{init} at P_{init} = 360 atm, and bottom points correspond to the final temperatures T_{fin} of an adiabatic expansion process at the specified final pressure of P_{fin} = 1 atm: (*a*) critical point of a two-phase equilibrium and (*b*) critical point of a three-phase equilibrium.

sition changes [37]. The boundaries of the parameter region in which a substance is released as a solid phase at the corresponding chemical composition of the starting mixture and at certain amounts and ratios between a solvent and an antisolvent in this mixture were calculated. The parameters of the critical point and fluid–solid boundary lines were calculated as applied to a mixture of ethanol, carbon dioxide, and phenanthrene ($C_{14}H_{10}$). Conditions for the separation of a mixture with a specified composition into solid, liquid, and gas phases were found, and the composition, amounts, and properties of each of the resulting equilibrium phases were determined (see Fig. 12). We found that the choice of the parameters of the supercritical state of a mixture plays a crucial role in the optimization of conditions for the formation of the solid phase in the course of the rapid adiabatic expansion of a fluid.

Treatment of a diamond mixture with supercritical water. Recently, attention has been focused on studies of carbon nanostructures. Among the various synthesized carbon nanomaterials, so-called ultradisperse nanodiamonds, which are obtained in the detonation of carbon-containing solid explosives with a negative oxygen balance, should be distinguished. The area of application of ultradisperse diamonds can be broad. Although the productivity of this technique is high, the resulting product (detonation soot or diamond mixture) contains various carbon structures and species. The concentration of a diamond phase in these products is about 35–45 wt %. As a rule, the starting mixture is treated at elevated pressure and temperature with liquid or gaseous oxidizing agents to separate the diamond phase and to remove water-insoluble impurities. Sulfuric acid and nitric acid mixtures, sulfur dioxide, and chromic anhydride are used as the oxidizing agents.

However, chemical purification with the use of strong acids can result, on the one hand, in the oxidation of the diamond phase and the surface contamination of diamonds with various functional groups and, on the other hand, in the release of a large amount of corrosive wastes. Thus, the problem was formulated to study the treatment of a detonation carbon mixture prepared at the FNPTs Altai (Biisk) both in supercritical water and in supercritical water with hydrogen peroxide added. The experiments were performed in an autoclave reactor in supercritical water at 390 ± 5°C and 285 ± 5 atm. After adjusting the temperature and pressure, the process was performed for 4 to 6 h.

The phase composition of the solid phase before and after the treatment of the mixture in supercritical water was studied by electron microscopy (HRTEM and SEM) and X-ray diffraction (XRD).

According to HRTEM data, the initial sample of the mixture—detonation carbon (Fig. 13a)—consisted of a uniform carbon material in terms of density with nanostructures of various types: amorphous carbon, onion carbon, and diamond nanocrystals.

The interaction of carbon from a mixture of nanodiamonds with supercritical water results in the formation of a large amount of gas products, mainly CO and CO_2, which suggest the deep oxidation of the carbon phase in supercritical water.

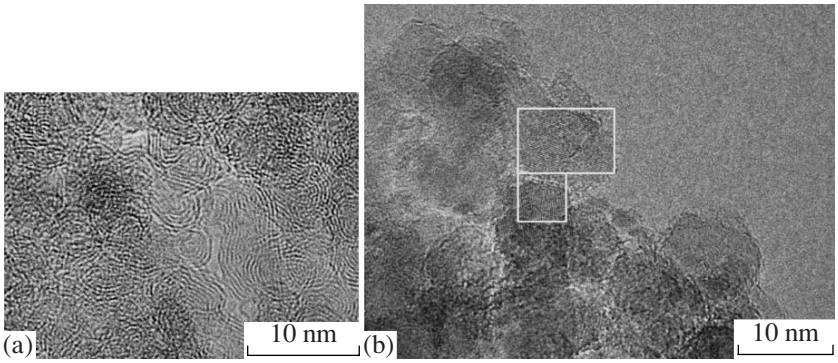

Fig. 13. HRTEM images of (a) a detonation carbon mixture and (b) the same mixture after treatment with supercritical water with the participation of hydrogen peroxide decomposition products.

An analysis of the HRTEM images of detonation carbon samples after treatment with supercritical water with the participation of hydrogen peroxide decomposition products indicated (Fig. 13b) that onion carbon was converted into graphene fibers, degraded, or oxidized. According to the results of XRD analysis, the fraction of the diamond phase in the samples treated with supercritical water increased from 34–45 to 75 wt %.

SIMULATION AND OPTIMIZATION OF PROCESSES AND REACTORS FOR CHEMICAL REACTIONS IN SUPERCRITICAL FLUIDS

Special features of physicochemical transformations under supercritical conditions should be taken into consideration in the mathematical simulation of processes, reactors, and process flowsheets in which chemical reactions occur in SCFs. Differences between the physicochemical and thermodynamic properties of SCFs and ideal gas atmospheres and the dependence of the kinetics of chemical reactions on the pressure (density) of the medium belong to these special features [19].

Oxidation of phenol in supercritical water in a perfectly mixed reactor. Ermakova et al. [38, 39] simulated a perfectly mixed reactor for the oxidation of phenol in supercritical water. The oxidation of phenol in supercritical water occurs by a complicated mechanism [40] with the formation of intermediates, such as acetic acid, which are subsequently oxidized to CO_2 and water. It is believed that adiabatic conditions occur in the reactor. Oxygen was used as an oxidizing agent, which was prepared by the decomposition of hydrogen peroxide in a heat exchanger upstream of the reactor:

$$C_6H_6O + 4O_2 \xrightarrow{\text{I(1Ph)}} \frac{3}{2}CH_3COOH + 3CO_2; \quad \text{(I)}$$

$$CH_3COOH + 2O_2 \xrightarrow{\text{II(Ac)}} 2CO_2 + 2H_2O; \quad \text{(II)}$$

$$C_6H_6O + 7O_2 \xrightarrow{\text{III(2Ph)}} 6CO_2 + 3H_2O. \quad \text{(III)}$$

The rate equations of reactions (I)–(III) were chosen based on published data [40, 41].

The mathematical model of the perfectly mixed reactor includes the material and thermal balance equations

$$F_i \equiv y_i^0 - \gamma y_i^{\text{out}} + q_i(T^{\text{out}}, P, \mathbf{y}^{\text{out}})\tau = 0 \quad (i = 1, 2, \ldots, N_S), \quad (21)$$

$$F_{N_S+1} \equiv \sum_{i=1}^{N_S} y_i^0 \overline{H}_i(\mathbf{y}^0, T^0, P) - \gamma \sum_{i=1}^{N_S} y_i^{\text{out}} \overline{H}_i(\mathbf{y}^{\text{out}}, T^{\text{ad}}, P) = 0. \quad (22)$$

Here,

$$\gamma \equiv N^{\text{out}}/N^0, \quad \gamma = 1 + \tau \sum_{i=1}^{N_S} q_i, \quad \tau \equiv V_R/N^0,$$
$$y_i^0 = n_i^0/N^0 \text{ and } y_i^{\text{out}} = n_i^{\text{out}}/N^{\text{out}} \quad (23)$$
$$\left(N^0 = \sum_{i=1}^{N_S} n_i^0 \text{ and } N^{\text{out}} = \sum_{i=1}^{N_S} n_i^{\text{out}} \right).$$

$q_i = \sum_{j=1}^{N_R} Z_{ji} R_j$ is the rate of formation/consumption of the ith mixture component (in mol l^{-1} s^{-1}); Z_{ji} is the element of the jth row and the ith column of the matrix of stoichiometric coefficients of chemical reactions; R_j is the rate of the jth chemical reaction in the reactor as a prescribed function of temperature, pressure (molar volume), molar fractions, and rate constants; n_i^0 and n_i^{out} are the molar flows of the ith mixture component at the reactor inlet and outlet, respectively (mol/s); $\mathbf{y}^{\text{out}}$ is the N_S-dimensional vector of the mole fractions of components in the reactor and, correspondingly, in the outgoing flow from the reactor; T^{out} is the temperature in the reactor and outgoing flow; P is the pressure in the

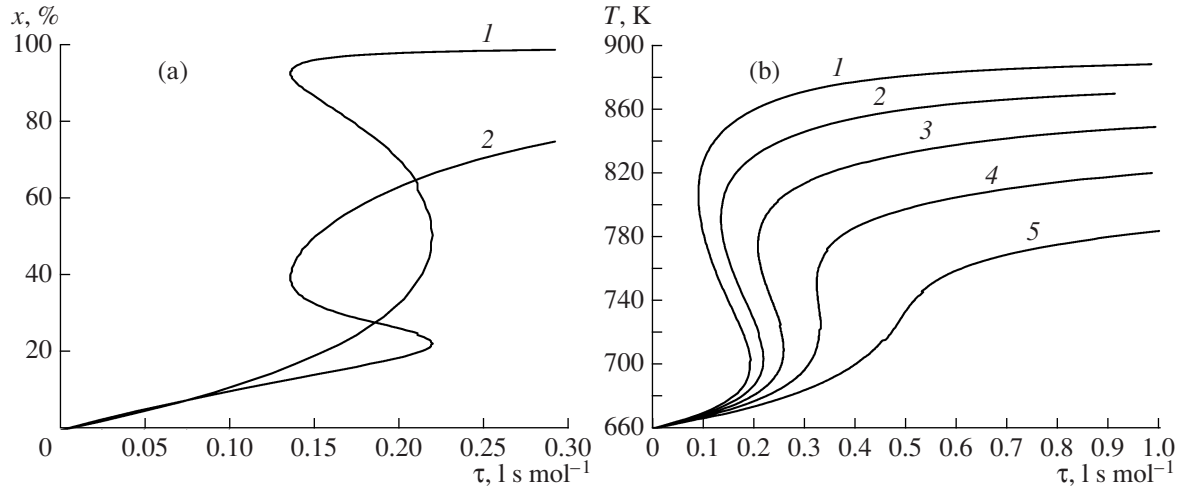

Fig. 14. Dependences of (a) the conversion of (*1*) methanol and (*2*) phenol and (b) the temperature of the reaction mixture in the reactor on the residence time at the following concentrations of methanol in the starting mixture, %: (*1*) 1.69, (*2*) 1.57, (*3*) 1.43, (*4*) 1.29, and (*5*) 1.09.

system; V_R is the reactor volume (l); and $\overline{H}_i$ are the partial molar enthalpies of the individual components (cal/mol). The molar volume of the mixture (l/mol) is designated by $V_{mix}(T, P, \mathbf{y}^{out})$.

The algorithm for solving this problem was based on the well-known arc-length integration method [42]. The contact time τ served as the continuation parameter. A two-step predictor–corrector algorithm with Euler predictor and Newton corrector steps was used.

In accordance with previous calculations [38, 39], the above model has three steady-state solutions, which can be demonstrated clearly using the dependence of the conversions of both initial or intermediate substances and reaction products on contact time as an example (Fig. 14a). Figure 14a shows the dependences of methanol and phenol conversions on τ. The shape of the dependences of the temperature of the adiabatic heating of a mixture at various initial methanol concentrations on contact times (Fig. 14b) also suggests a multiplicity of steady states. Numerical analysis demonstrated that the multiplicity of solutions depends on the nonlinear behavior of the heat capacity of the reaction mixture in the critical region of parameters and on the presence of methanol in the starting mixture.

Simulation and optimization of process parameters for the oxidation of organic compounds in supercritical water. Ermakova and Anikeev [43] considered a process flowsheet for the oxidation of acetic acid with hydrogen peroxide in supercritical water; this flowsheet served as a prototype for a pilot plant. On the one hand, acetic acid chosen as a reagent is a target or intermediate compound in decomposition reactions of many organic substances. On the other hand, it participates in a rate-limiting step of the process. Methanol dissolved in water served as a fuel, and hydrogen peroxide served as an oxidizing agent.

The mathematical models of the individual components of the process flowsheet are coupled to each other by mass and heat flows. Each particular model takes into account special features of processes occurring under supercritical conditions: changes in the thermodynamic properties (enthalpy, heat capacity, and critical parameters) of the reaction mixture depending on the pressure, temperature, and composition of this mixture at various points along the apparatus.

The main reaction paths in the transformations of the participants of acetic acid oxidation in supercritical water (reactions (I)–(III)) are given above. The model equations have the following forms:

$$\frac{dy_i}{d\tau} = \frac{1}{\gamma}\left[q_i - y_i\frac{d\gamma}{d\tau}\right] \quad (i = 1, 2, \ldots, N); \tag{24}$$

$$\frac{dT}{d\tau} = \frac{1}{\gamma\bar{c}_p}\left[-\sum_{i=1}^{N}(q_iH_i) - \bar{c}_pT\frac{d\gamma}{d\tau}\right]; \tag{25}$$

$$\frac{d\gamma}{d\tau} = \sum_{i=1}^{N} q_i, \quad q_i = \sum_{j=1}^{N_R} Z_{ji}R_j. \tag{26}$$

Initial conditions (at $\tau = 0$):

$$F = F^0, \quad \gamma = 1, \quad y_i = y_i^0, \quad T = T^0, \quad \bar{c}_p = \bar{c}_p(T^0). \tag{27}$$

Here, $\gamma \equiv F/F^0$, $\tau \equiv V/F^0$; F^0, T^0, and y_i^0 are the flow characteristics at the reactor inlet; F is the substance flow (mol/s); y_i ($i = 1, 2,\ldots, N$) is the mole fraction of the ith component; q_i is the rate of conversion (formation) of the ith component (mol l^{-1} s^{-1}).

The calculation and optimization of the process flowsheet should mainly demonstrate the main special features of chemical reactions in supercritical water as a solvent. Ermakova and Anikeev [43] also studied the effects of entry parameters, fuel and oxidant concentrations, and process conditions in particular units of the flowsheet on the complete oxidation of acetic acid at minimum apparatus sizes.

Effect of the imperfection of the reaction mixture on the Fischer–Tropsch synthesis in a supercritical solvent. With the use of published data on the kinetics of the Fischer–Tropsch reaction in the presence of a commercial catalyst based on iron oxide, Ermakova et al. [44] constructed a kinetic model taking into consideration the effect of the nonideal reaction mixture on the rate of the reaction. The imperfection was taken into account using fugacity coefficients, which were calculated from a modified RKS equation of state. The Schulz–Flory distribution equations were derived for saturated and unsaturated hydrocarbons as functions of the fugacity of CO and H_2 in the reaction mixture. The model proposed describes the reaction kinetics in the temperature range of 523–623 K and the pressure range of 6–100 atm. Based on the calculation of critical parameters of the mixture, a method of fitting the nature and optimum concentration of a supercritical solvent was proposed. A comparative analysis of processes occurring in a supercritical solvent and in the absence of a solvent was performed. It was found that the reaction rate and the total yield of C_2^+ olefins, including a target fraction of C_5–C_{11}, can be considerably increased under supercritical conditions.

OXIDATION OF TRINITROGLYCEROL AND DIETHYLENE GLYCOL DINITRATE IN SUPERCRITICAL WATER

The results of the studies of the reaction kinetics and thermodynamics and mathematical simulation were used in the design of a pilot plant for complete oxidation of a mixture of trinitroglycerol and diethylene glycol dinitrate, which are wastes from explosive manufacturing processes, in supercritical water [45]. The plant with a throughput of 30–40 l/h with a tubular reactor was developed at the FNPTs Altai. Hydrogen peroxide, air, or a combination of air with ammonium nitrate served as an oxidizing agent. Acetone was chosen as a fuel.

The degree of oxidation of trinitroglycerol and diethylene glycol dinitrate was 99.9–100% in the majority of regimes. The plant was stable in operation in a controllable mode.

With the use of air for the oxidation of nitro esters in supercritical water in all of the regimes, the complete oxidation of the nitro ethers was performed over the temperature range of 414–689°C. At the same time, a temperature higher than 600°C was required for the complete oxidation of acetone to carbon dioxide and water.

Atmospheric oxygen and ammonium nitrate were used as oxidizing agents for the oxidation of complex organic wastes. The initial concentration of organic wastes in water was 9.1% (including 65–75% dimethylformamide, 15–25% acetic acid, 4–10% ethanol, 2–5% toluene, and up to 10% unidentified impurities), and the concentration of an inorganic oxidant (ammonium nitrate) in the initial solution was 1.7%. Ammonium nitrate was a good oxidizing agent for organic compounds.

The tests demonstrated the high efficiency of decomposition and oxidation of a wide variety of organic wastes from explosive manufacturing processes in supercritical water.

In this publication, only a small portion of our studies that demonstrate the efficiency and promise of the use of SCF solvents for the chemical conversion of organic compounds is considered. Heterogeneous and homogeneous catalytic reactions, as well as biological processes, in SCFs are of considerable interest. Unique results can be obtained in the chemistry of polymers in supercritical solvents. Studies in all of the above areas are in progress, and new interesting results will inevitably be obtained.

REFERENCES

1. Savage, P.E., *Chem. Rev.*, 1999, vol. 99, p. 603.
2. *Chemical Synthesis Using Supercritical Fluids*, Jessop, P.G. and Leitner, W., Eds., Weinheim; Wiley-VCH, 1999.
3. Abeln, J., *Environ. Eng. Sci.*, 2004, vol. 21, no. 4, p. 93.
4. Savage, E.P., Gopalan, S., Martino, Ch.J., and Brock, E.E., *AIChE J.*, 1995, vol. 41, p. 1723.
5. Anikeev, V.I., Yermakova, A., Manion, J., and Huie, R., *J. Supercrit. Fluids*, 2004, vol. 32, p. 123.
6. Anikeev, V.I., Ermakova, A., and Goto, M., *Kinet. Katal.*, 2005, vol. 46, no. 6, p. 868 [*Kinet. Catal.* (Engl. Transl.), vol. 46, no. 6, p. 821].
7. Marquardt, D.W., *J. Soc. Ind. Appl. Math.*, 1963, vol. 11, p. 431.
8. Yermakova, A. and Anikeev, V., *Ind. Eng. Chem. Res.*, 2000, vol. 39, p. 1453.
9. Soave, G., *Chem. Eng. Sci.*, 1972, vol. 27, p. 1197.
10. Anikeev, V.I. and Ermakova, A., *Teor. Osn. Khim. Tekhnol.*, 1998, vol. 32, no. 5, p. 508 [*Theor. Found. Chem. Eng.* (Engl. Transl.), vol. 32, no. 5, p. 462].
11. Anikeev, V.I., Ermakova, A., Golovizin, A.V., and Goto, M., *Zh. Fiz. Khim.*, 2004, vol. 78, no. 10, p. 1791 [*Russ. J. Phys. Chem. A* (Engl. Transl.), vol. 78, no. 10, p. 1553].
12. Krichevskii, I.R., *Fazovye ravnovesiya v rastvorakh pri vysokikh davleniyakh* (Phase Equilibria in Solutions at High Pressures), Moscow: Goskhimizdat, 1952.
13. *Termodinamika ravnovesiya zhidkost'-par* (Thermodynamics of Liquid–Vapor Equilibria), Morachevskii, A.G., Ed., Leningrad: Khimiya, 1980.

14. Ermakova, A. and Anikeev, V.I., *Teor. Osn. Khim. Tekhnol.*, 2000, vol. 34, p. 57 [*Theor. Found. Chem. Eng.* (Engl. Transl.), vol. 34, p. 51].

15. Ermakova, A., Fadeev, S.I., and Anikeev, V.I., *Zh. Fiz. Khim.*, 2001, vol. 75, no. 8, p. 1394 [*Russ. J. Phys. Chem. A* (Engl. Transl.), vol. 75, no. 8, p. 1266].

16. Ermakova, A. and Anikeev, V.I., *Teor. Osn. Khim. Tekhnol.*, 1999, vol. 33, p. 62 [*Theor. Found. Chem. Eng.* (Engl. Transl.), vol. 33, p. 56].

17. Ermakova, A., Sazhina, O.V., and Anikeev, V.I., *Teor. Osn. Khim. Tekhnol.*, 2005, vol. 39, p. 88 [*Theor. Found. Chem. Eng.* (Engl. Transl.), vol. 39, p. 85].

18. Michelsen, M.L., *Fluid Phase Equilib.*, 1982, vol. 9, p. 21.

19. Ermakova, A., Golovizin, A.V., and Anikeev, V.I., *Zh. Fiz. Khim.*, 2004, vol. 78, no. 11, p. 1938 [*Russ. J. Phys. Chem. A* (Engl. Transl.), vol. 78, no. 11, p. 1723].

20. Sandler, S.I., *Chemical and Engineering Thermodynamics*, Chichester: Wiley, 1999, 3rd ed.

21. Anikeev, V.I., Manion, D., Ermakova, A., and Huie, R., *Kinet. Katal.*, 2002, vol. 43, no. 2, p. 209 [*Kinet. Catal.* (Engl. Transl.), vol. 43, no. 2, p. 189].

22. Anikeev, V.I., Goto, M., and Yermakova, A., *Proc. Int. Congr. Supercritical Fluids*, Versailles, 2003, vol. 2, p. 1307.

23. Anikeev, V.I., Yermakova, A., and Goto, M., *Ind. Eng. Chem. Res.*, 2004, vol. 43, p. 8141.

24. Anikeev, V.I., Yermakova, A., Semikolenov, V.A., and Goto, M., *J. Supercrit. Fluids*, 2005, vol. 33, p. 243.

25. Anikeev, V.I., Ermakova, A., Chibiryaev, A.M., Kozhevnikov, I.V., and Mikenin, P.E., *Zh. Fiz. Khim.*, 2007, vol. 81, no. 5, p. 825 [*Russ. J. Phys. Chem. A* (Engl. Transl.), vol. 81, no. 5, p. 711].

26. Fuguitt, R.E. and Hawkins, J.E., *J. Am. Chem. Soc.*, 1945, vol. 67, p. 242.

27. Gajewski, J.J., Kuchuk, I., Hawkins, C., and Stine, R., *Tetrahedron*, 2002, vol. 58, p. 6943.

28. Crowley, K.J. and Traynor, S.G., *Tetrahedron*, 1978, vol. 34, p. 2783.

29. Gajewski, J.J. and Hawkins, C.M., *J. Am. Chem. Soc.*, 1986, vol. 108, p. 838.

30. Yermakova, A., Chibiryaev, A.M., Kozhevnikov, I.V., Mikenin, P.E., and Anikeev, V.I., *Chem. Eng. Sci.*, 2007, vol. 62, p. 2414.

31. Ermakova, A., Chibiryaev, A.M., Mikenin, P.E., Sal'nikova, O.I., and Anikeev, V.I., *Zh. Fiz. Khim.*, 2008, vol. 82, no. 1, p. 62 [*Russ. J. Phys. Chem. A* (Engl. Transl.), vol. 82, no. 1, p. 62].

32. Chibiryaev, A.M., Ermakova, A., Kozhevnikov, I.V., Sal'nikova, O.I., and Anikeev, V.I., *Izv. Akad. Nauk, Ser. Khim.*, 2007, no. 5, p. 1188.

33. Anikeev, V.I. and Ermakova, A., *Zh. Fiz. Khim.*, 2003, vol. 77, no. 2, p. 265 [*Russ. J. Phys. Chem. A* (Engl. Transl.), vol. 77, no. 2, p. 211].

34. Anikeev, V.I., Menion, D., and Ermakova, A., *Zh. Fiz. Khim.*, 2001, vol. 75, no. 8, p. 1387 [*Russ. J. Phys. Chem. A* (Engl. Transl.), vol. 75, no. 8, p. 1259].

35. Narayan, R. and Antal, M.J., *J. Am. Chem. Soc.*, 1990, vol. 112, p. 1927.

36. Johnson, K.P. and Haynes, C., *AIChE J.*, 1987, vol. 33, p. 2017.

37. Anikeev, V.I. and Ermakova, A., *Zh. Fiz. Khim.*, 2007, vol. 81, no. 12, p. 2245 [*Russ. J. Phys. Chem. A* (Engl. Transl.), vol. 81, no. 12, p. 2024].

38. Ermakova, A., Mikenin, P.E., and Anikeev, V.I., *Teor. Osn. Khim. Tekhnol.*, 2006, vol. 40, no. 2, p. 168 [*Theor. Found. Chem. Eng.* (Engl. Transl.), vol. 40, p. 168].

39. Yermakova, A. and Anikeev, V.I., *Chem. Eng. Sci.*, 2005, vol. 60, p. 3199.

40. Krajnc, M. and Levec, J., *AIChE J.*, 1996, vol. 42, p. 1977.

41. Lixiong, Li., Peishi, Chen., and Gloyna, E.F., *AIChE J.*, 1991, vol. 37, p. 1687.

42. Choi, S.H., Harney, D.A., and Book, N.L., *Comput. Chem. Eng.*, 1996, vol. 20, p. 647.

43. Ermakova, A. and Anikeev, V.I., *Teor. Osn. Khim. Tekhnol.*, 2004, vol. 38, no. 4, p. 355 [*Theor. Found. Chem. Eng.* (Engl. Transl.), vol. 38, no. 4, p. 333].

44. Ermakova, A., Anikeev, V.I., and Froment, Dzh.F., *Teor. Osn. Khim. Tekhnol.*, 2000, vol. 34, no. 2, p. 203 [*Theor. Found. Chem. Eng.* (Engl. Transl.), vol. 34, no. 2, p. 180].

45. Anikeev, V.I., Belobrov, N.S., Piterkin, R.N., Prosvirnin, R.Sh., Zvolsky, L.S., Mikenin, P.E., and Yermakova, A., *Ind. Eng. Chem. Res.*, 2006, vol. 45, p. 7977.